THE PHYSICAL PROPERTIES OF A SET OF SANDSTONES, III: THE EFFECTS OF FINE GRAINED PORE FILLING MATERIAL ON COMPRESSIONAL WAVE VELOCITY

R.H. Wilkens*, G. Simmons, T.M. Wissler and L. Caruso

Earth Resources Laboratory*
and
Department of Earth and Planetary Sciences
Massachusetts Institute of Technology
Cambridge, MA 02139

ABSTRACT

We have used aspect ratio modeling to explain the measured compressional wave velocities of twenty different dry sandstone samples with varying clay contents at a single confining pressure of 0.5 kbar. Velocities of the sandstones range between 3.1 km/sec and 5.7 km/sec. Measured porosities are between 6% and 33%, clay contents between 2% and 30%. Pores were described using three simple type classifications. The pore type distributions of the samples were quantified by point counting polished impregnated thin sections using a scanning electron microscope. A representative aspect-ratio was assigned to each of the three categories of pore type. Velocities were modeled using these aspect ratios weighted by the observed distribution of the porosity types. Agreement between theoretical and measured velocities is generally within 10%. The modeling suggests that the effects of clays in sandstone pores is to reduce the sample porosity without reducing the non-framework (void + clay) volume. Thus, for a given porosity, clay rich samples contain greater non-framework volume, which in turn lowers velocity. The model derived from the dry measurements can be used to successfully approximate empirical relationships for saturated samples of velocity-porosity-clay content taken from the literature.

INTRODUCTION

The physical properties of porous rocks are governed to a large extent by the geometry and volume of their pores. In recent years parallel theoretical and observational studies have helped to develop a better understanding of the effects of pores on properties such as acoustic velocity and permeability (Pittman, 1984, Seeburger and Nur, 1984). There remains, however, the need to bridge the gap between the thin section observations of the sedimentary petrologist and the laboratory data and formulations of the rock mechanic. It is the purpose of this study to integrate measurements of V_p in the laboratory, direct SEM observations of pores, and aspect ratio modeling of sandstone velocity. Twenty different sandstone samples were chosen; each composed predominantly of quartz grains and varying in total porosity and in the amount of clay and fine grained material present. In this manner the variables to be considered during modeling are reduced. For each sample we measured V_p of dry cores to 1.0 kbar and described the pores using a simple system of classification. Pore types were assigned specific aspect ratios and velocities were calculated using pore aspect ratio modeling. Aspect ratio values were determined which produce agreement between computed V_p and measured

values of V_p at a confining pressure of 0.5 kbar.

Laboratory studies of the compressional wave velocities (V_p) of sandstones have been carried out for over three decades. Early studies attempted to establish regular empirical relationships between velocity and other properties such as density, porosity or the nature of the pore filling material (Wyllie, et al., 1956). It was recognized that confining pressure also had a significant effect on V_p in laboratory experiments (Wyllie, et al., 1958). Birch (Birch, 1960, Birch, 1961) suggested that most of the V_p-pressure dependence in low porosity igneous and metamorphic rocks was due to the closure of flat cracks within the samples at elevated pressures. Walsh (Walsh, 1965, Walsh, 1969) provided theoretical formulations to model the effects of both dry and saturated cracks in low porosity rocks on rock properties.

The scanning electron microscope (SEM) allowed investigators to view in great detail the geometry of pore space within a wide variety of rock types (Pittman and Duschatko, 1970, Timur, et al., 1971). The increased sophistication in crack and pore observation was matched by more complex theoretical work which predicted rock properties based on porosity, pore space geometry and pore fluid properties (Kuster and Toksöz, 1974, Part I, Kuster and Toksöz, 1974, Part II, O'Connell and Budiansky, 1974). These studies generally matched theoretical crack distributions to laboratory V_p measurements for single samples over an interval of changing confining pressure. Cheng and Toksöz (Cheng and Toksöz, 1979) inverted velocity-pressure data for single samples to obtain a pore aspect ratio distribution. (The aspect ratio is the ratio of the minor to major axis of a spheroid and thus a measure of flatness.) Recent laboratory studies have examined the effects of pore filling materials such as clay and fine grained detritus on V_p (De Martini, et al., 1976, Tosaya and Nur, 1982, Kowallis, et al., 1985). These studies developed empirical relationships of V_p-clay content-porosity for both dry and saturated samples which indicated that the presence of fine grained material in sandstones lowers V_p.

EXPERIMENTAL PROCEDURES

Three orthogonal samples, 2.5 cm in diameter and from 3 to 7 cm in length were cored from each of twenty sandstones. Where bedding was visible in the hand specimens, one core was cut with its axis normal to bedding, the other two with their axes in the plane of the bedding. Total sample volumes were calculated from core dimensions and grain volumes were measured using an air comparison pycnometer. After weighing, values of bulk density, grain density, and porosity were calculated. Samples were dried for 48 hours in a vacuum oven, jacketed in copper foil, and stored in dessicators. Velocities of compressional waves (V_p) were measured with 1.0 MH_z lead zirconium titanate transducers as a function of hydrostatic pressure to 1.0 kb for most samples using the pulse transmission technique of Birch (Birch, 1960). Several of the cores from less competent specimens failed (crushed) between 0.5 and 1.0 kb. Dry cores were used in the study to accentuate the effects of pores on the measured velocity.

A complete description of the samples used in this study and a discussion of their pores is presented in Caruso, et al. (Caruso, et al., 1985). We used a scheme adapted from standard petrographic terminology (Selley, 1982) to describe our sandstones. A sandstone is composed of grains, cement, matrix, and pores. Grains are the relatively large detrital particles which in our sample set are mostly quartz. Cement is post depositional mineral growth. Grains and cement constitute the

framework of our sandstones. Matrix is the finer material which occurs within the non-framework volume and pores are the open areas not occupied by framework or matrix. It should be noted that the term "matrix" has different definitions in different disciplines. Useage in this study is consistent with petrographic description. Rock mechanics commonly uses "matrix" to describe the continuous solid volume of a sample, the "framework" of this study. While this distinction may create initial confusion, it is worthwhile to adopt accepted descriptive terminology when combining observation and theory.

The non-framework volume was divided into three categories: (1) intergranular pores - high aspect ratio volumes containing no filling material, (2) Matrix regions - those volumes, typically intergranular pores, which have been partially filled with clay and fine grained material and contain both matrix and the very small pores we term micropores, and (3) connective pores - low aspect ratio micron width crack-like pores which generally exist at grain to grain contacts. The categories are illustrated in figure 1. One impregnated polished thin section from each sandstone was examined using a scanning electron microscope (SEM). Each thin section was point counted on the SEM until approximately 300 non-framework counts were recorded. The results of point counting determined the non-framework volume within each sample. These volumes ranged from near 10% to over 45%. Non-framework volumes, which include both pore volume and matrix volume, were then compared to sample porosities measured with the air comparison pycnometer. A linear regression between the two data sets suggested that the actual void volume within matrix regions (which we term microporosity) is approximately 50% (Caruso, et al., 1985).

The pore distribution data are plotted on a ternary diagram representing the three pore types in figure 2. Point counts of microporosity zones were reduced by 50% to adjust for grain volume. Values at each location are the average measured porosities for the three cores of each sandstone. Values for the per cent volume of each of the three types of porosity can be obtained by multiplying the total porosity by the abundance of each pore type. The volume of matrix regions , including both fine grained material and micropores, is equal to two times the micropore volume.

The difference between microporosity and the volume of matrix regions is significant in that thin section point counting techniques commonly yield clay content values which are equivalent to matrix region volumes, whereas electric and nuclear logs measure separately the microporosity , as part of the total porosity, and clay content values which reflect only the volumetric abundance of clay matrix grains. Thus point count breakdowns of rock fabric are not directly applicable to log measurements.

RESULTS

Velocity-Porosity

Values of density, porosity, and V_p are presented in Table 1. The value of V_p at 0.5 kb confining pressure is plotted versus the measured porosity of each core in figure 3. Porosities range between 6% and 33% and velocity varies between 3.1 km/sec and 5.7 km/sec. Scatter in the data represents both the differences between the various sandstones and the inhomogeneity and anisotropy encountered in measuring values of three adjacent cores from a single sample. Because this inhomogeneity exists on a scale of centimeters in our samples we use average

values of the three determinations for our analysis; assuming that this will be more representative of whole rock values than the results from any single core.

The line on figure 3 represents the Wyllie time average equation (Wyllie, et al., 1958) computed using a quartz matrix (V_p = 6.05 km/sec) and air in the pore spaces (V_p =0.34 km/sec). All of the measured values plot well below the time average line, in agreement with the observations of previous investigators that the presence of clay in a sample lowers the value of V_p (De Martini, et al., 1976, Tosaya and Nur, 1982, Kowallis, et al., 1985). The volume in our samples that is occupied by clay, other fine grained material and the microporosity included in these aggregates ranges from 2% to 30%.

Modeling-Theoretical Results

Previous studies have presented empirical relationships between V_p, porosity, and clay content at several different pressures for both dry and saturated rocks. They represent valuable demonstrations of the nature of the effect of clay on V_p. However, they do not answer the central question of defining the mechanism which causes the observed effect. This problem is best examined by employing a mechanical model of sandstone behavior in conjunction with pore type quantification. Pore aspect ratio modeling (Kuster and Toksöz, 1974, Part I, Kuster and Toksöz, 1974, Part II, Toksöz, et al., 1976, Cheng and Toksöz, 1979) has been used to describe successfully velocity-pressure relationships for single samples through inversion schemes. Wilkens, et al. (Wilkens, et al., 1984) have used theoretical velocity-porosity relationships derived from this model to relate measured velocity to SEM pore examination of siliceous limestones. We use pore aspect ratio modeling here to demonstrate the effect of matrix materials on V_p.

There are three important components of the modeling scheme we are using:

(1) Modeling V_p of a variety of samples measured at a constant confining pressure. Pore aspect ratio modeling as well as other modeling schemes, has generally been used to invert velocity-pressure data from a single sample to solve for some sort of pore geometry parameter(s). Our aspect ratios are inputs to the model; not results.

(2) Assuming that a given type of pore has a constant aspect ratio for all samples studied. The framework moduli and density used are those of quartz (K=0.37Mb,μ=0.45Mb,ρ=2.65gm/cc). Thus we are considering simple distributions of three aspect ratios in a quartz framework.

(3) Computing velocities by forward modeling of the observed pore type distribution .The predicted velocities reflect the three aspect ratios chosen to represent intergranular (α_I), connective (α_C), and microporosity (α_M); their relative distribution within a given sample (figure 2); and the total porosity of that sample, which determines the net volumetric abundance of each aspect ratio (pore type).

We have plotted the average value of V_p from each sample next to its location on the pore geometry ternary diagram in figure 4a. There is no regularity or trend evident in these data since the velocity is controlled not only by the relative abundance of porosity types; but also by the total porosity of each individual sample.

As a first attempt at modeling these data, we make the assumption of spherical pores, with the aspect ratios of all three pore types being equal to 1.0. ($\alpha_I = \alpha_C = \alpha_M = 1.0$). The values plotted in figure 4b represent the ratio of the actual measured velocity (figure 4a) to the velocity predicted using the spherical pore assumption. All of these ratios are less than 1.0, indicating that for every sample the velocity measured was less than the velocity calculated; by anywhere from 10 to 40%. This is not surprising in view of the fact that aspect ratio modeling with spherical pores behaves very much like the time average line of figure 3, which also predicts velocities greater than measured values. Furthermore, our SEM observations reveal that, in the case of connective pores, α_C should be much less than unity.

Before modeling further the measured data it is useful to illustrate the effect on predicted velocities of both aspect ratio distribution and total sample porosity. We have calculated velocity contours for theoretical samples of 10 and 20% porosity assuming that this porosity is distributed among α values of 1.0 (spherical), 0.1 (10 to 1 flattening), and 0.025 (40 to 1 flattening). The results are displayed on ternary diagrams in figure 5. The 10% porosity example (figure 5a), shows that a flattening of pores reduces V_p and that for samples of identical total porosity the distribution of aspect ratios is an important control of V_p. A sample containing 10% pores of $\alpha = 1.0$ would have a value of $V_p \approx 5.8 km/sec$. For 10% of pores of $\alpha = 0.1, V_p \approx 4.8$ km/sec. If the sample had 5% pores of $\alpha = 1.0$ and 5% of $\alpha = 0.1$, then $V_p \approx 5.3$ km/sec. The theoretical model fails for a sample of 10% of $\alpha = 0.025$. Looking at the side connecting the $\alpha = 1.0$ and $\alpha = 0.025$ pores we see that for a mixture of these two aspect ratios, the theory can accomodate only about 65% of $\alpha = 0.025$ pores or 6.5% of the total rock volume (.65 x 10% porosity = 6.5%).

For a total porosity of 20% (figure 5b) the velocity contours lie further from the $\alpha = 0.025$ vertex. The aspect ratio distribution can contain only about 32.5% pores of $\alpha = 0.025$, or again 6.5% of the total rock volume (.325 x 20% porosity = 6.5%). Wyllie et al. (Wyllie, et al., 1958) noted that vugular porosity (i.e. semi-spherical) did not seriously effect the value of V_p. This is seen in our models. A sample containing 20% pores of $\alpha = 1.0$ has $V_p \approx 5.7$ km/sec, which is not much lower than the 10% pores of $\alpha = 1.0$ at $V_p = 5.8$ km/sec (figure 5a). However, for 20% porosity of $\alpha = 0.1, V_p \approx 3.7$ km/sec (figure 5b), a significant reduction when compared to V_p=4.9 km/sec for the 10% porosity of $\alpha = 0.1$ model (figure 5a).

These two models illustrate the importance of both the aspect ratio distribution (position on the ternary) and the total sample porosity in predicting V_p. However for any single sample of a given porosity, pore type distribution, and measured V_p; the choice of aspect ratios is non-unique. The important concept of our approach is using a single set of α – pore type pairs for all of our data. Each predicted velocity will represent a combination of the effects of the same three aspect ratios, weighted by their relative abundance as determined from direct observation and by the total measured porosity of the individual sample.

Modeling-Theory vs Observation

The spherical pore model (figure 4b) was not satisfactory as we over-predicted V_p in every case. Our technique in modeling the experimental results is to perturb the effective aspect ratios assigned to intergranular, connective, and microporosity until we have found a combination of α_I, α_C, and α_M which will adequately predict V_p

for all of our samples. We know from the theoretical results (figure 5) that decreasing values of α will reduce predicted velocities.

Observation tells us that the connective pores in particular should not be represented by $\alpha_C = 1.0$, so we hold α_I and α_M to 1.0 and reduce α_C in stages to examine the effects of this change on the ratio of measured to predicted V_p (figure 6). Little change is observed when $\alpha_C = 0.1$, all predicted values of V_p are still too large although those samples richest in connective porosity do show a somewhat better fit. Reducing α_C to 0.05 provides a better fit for many of the measured values, yet they are still less than the predicted V_p. At $\alpha_C = 0.025$, 13 of the measured values are within 10% of predicted V_p and a single sample has a measured V_p greater than the predicted value. A final reduction, to $\alpha_C = 0.01$, results in the model being unable to predict V_p for 9 samples due to the limitations discussed above on the total volumetric abundance of very flat pores. It is worth noting that three of these samples fall amongst others which have not reached this limit, a reflection of the interaction of both position on the ternary diagram and total sample porosity in predicting V_p.

Examining the results of $\alpha_C = 0.025$, $\alpha_I = \alpha_M = 1.0$ (figure 6) there appears to be a general trend towards increasing misfit of the data away from the α_C vertex. Values of α_I and α_M were reduced together holding α_C constant at 0.025 (figure 7). Changing from $\alpha_I = \alpha_M = 1.0$ to $\alpha_I = \alpha_M = 0.5$ improves the goodness of fit to the data. This combination of pore aspect ratios predicts V_p of 15 of the samples to 10% of the measured V_p. A reduction to $\alpha_I = \alpha_M = 0.25$ fits 17 of the data; another small improvement. Further lowering of α_I and α_M to 0.15 indicates that we are now seriously under-predicting V_p for 12 of the samples and that the fit gets worse as we approach the connective vertex. After several more iterations we achieve a final result displayed in figure 8. The combination of $\alpha_I = 0.15$, $\alpha_M = 0.125$, and $\alpha_C = 0.05$ allows us to fit V_p for 19 of our 20 samples to 10%, 13 of which are within 5% of the measured values.

The Effect of Clay

We have used direct observation of pores and a mechanical model of sandstone behavior to adequately model V_p data of samples representing a range of porosities and matrix contents. However, our final result (figure 8) is intuitively unsettling. There is only a factor of three difference between α_I and α_C in the relative values of the final aspect ratio combination. Even though these values are an effective representation of what in reality must be a spectrum of aspect ratios, our SEM observations suggest that the difference should be greater. Second, the difference between α_I and α_M is trivial given the other variations in the measured data such as anisotropy and inhomogeneity; even though the work of previous investigators illustrates that the presence of clay (microporosity) influences velocity. The results suggest that there is very little difference between the two porosity types.

The apparent independence of the matrix in the pore spaces can be explained by assuming that in our dry samples the matrix is essentially decoupled from the rock framework. This is intuitively pleasing since SEM examination of the samples suggest that there is probably very little strength in the clay aggregates. Since these aggregates are essentially 50% air and 50% grain, they are probably ineffective in transmitting strain. We have used measured porosities throughout the process to be

consistent with porosity values measured by downhole logging tools. The modeling program assumes that whatever is not porosity is framework. However, the volume of microporosity in each sample is matched by an equal volume of matrix (clay or other fine grained material) that we believe is decoupled from the framework. This hypothesis can be tested by changing from a porosity (void volume) model to a non-framework (void + matrix volume) model. We have calculated non-framework volumes and displayed them on our ternary diagram in figure 9. Samples which are relatively clay-free show only small increases between porosity and non-framework volumes while those rich in clay have large increases.

The result of a second set of modeling iterations, with aspect ratio values weighted by pore and matrix distribution and total non-framework volume is presented in figure 10. V_p is predicted to within 10% for 18 of 20 samples using $\alpha_I = \alpha_M = 0.225$ and $\alpha_C = 0.05$. The value of α_C has not changed between the porosity and non-framework models, suggesting that the presence of matrix in the samples does not seriously effect the response of the connective pores. The values of α_I and α_M have increased to counteract the increase in non-framework volume of the samples modeled. The volumes of intergranular pores that are partially filled with matrix have the same effect as true intergranular pores. Also, the increase in α_I and α_M yields a much more satisfying relationship between their value and that of α_C. The connective pores are represented by a flattening of 20 to 1 whereas the larger pores (filled, partially filled, or empty) can be effectively modeled using a flattening of approximately 4 to 1. This is more consistent with SEM observations.

We may now address the central issue of the mechanism through which the presence of clay in sandstones lowers the velocity. Previous investigations have suggested that the clay aggregates add a low aspect ratio component to the framework of the sample (Kowallis, et al., 1985) or that dispersed clays lower the framework modulus due to their location between grains (Tosaya and Nur, 1982). Our modeling does not support this. Were α_M significantly lowered with respect to α_I the model would no longer fit most of our data. The fact that the modeling can essentially ignore clay in the non-framework volume suggests another, much simpler explanation that is more a problem of how the data have been considered than how clays interact with a sandstone framework.

The true effect of clays in sandstones is to occupy space. Because past studies have considered sandstones of equal porosity and varying clay contents they have neglected the central issue of framework and non-framework volume. Samples containing equal porosity and varying clay content have varying non-framework volume. As the matrix content increases, so too does the non-framework volume. It is this matrix volume increase which lowers velocity, not some intrinsic effect of the matrix itself on the framework moduli of the sandstone. Tosaya and Nur (Tosaya and Nur, 1982) observed that the velocity-clay content relationship did not depend on clay composition. This is logical if it is only the volume of that material which is important.

DISCUSSION

The Method

It is useful to discuss some of the limitations inherent in our method before moving on to some final speculations. The first is the problem of inhomogeneity and

anisotropy in our samples. In some cases cores cut immediately adjacent to each other from the same sample had markedly different porosities (Table 1), despite the fact that in hand specimen they appeared reasonably homogeneous. In point counting a single thin section from each sample we are assuming that the pore type distribution in each core is the same even though total porosity differs. The use of average values should alleviate this problem somewhat, but it probably contributes to scatter in our results. However, the fact that the modeling has been successful suggests that within limits these factors can be discounted.

Another problem is in the process of point counting. Point counting is subjective and almost sure to contain operator bias. In samples with high porosities predicted values of V_p are extremely sensitive to the relative amount of connective pores (see figure 5b). Differences of as little as 5% in the relative connective pore volume can greatly change predictions. It should be kept in mind that pore type distribution is dependent on the criteria employed during point counting.

A third problem is that of pressure. Pore distributions and porosity values determined for samples at atmospheric pressure have been used to describe velocity behavior at 0.5 kb. Aspect ratio modeling theory tells us that many flat cracks close over the pressure interval of 1.0 bar to 0.5 kb. Strain data collected over this pressure interval for our samples bear this out (Wissler and Simmons, 1985). Duplicating this effect in modeling would require a reduction in porosity (less than 1%) and probably some small shift in sample location on the ternary diagram. The best fit pore aspect ratio values might change somewhat, but not so much that they would change any of the conclusions of the present study.

Modeling the velocity-pressure data for all of our samples with single pore type-aspect ratio-pressure triplets is a logical step in this investigation. It will require the management of a much larger data set and as such represents a significant study in its own right which we choose not to address at this point; other than to realize the implications for the present work.

Use of the Model

The real strengths of using models rather than empirical relationships are twofold. First, they help to better understand mechanisms of variation. This has been illustrated by discussion of porosity versus non-framework volume. Second, a useful model should be able to predict behavior of a system in different states. Aspect ratio modeling has been used with single sample velocity-pressure data to model both dry and saturated behavior (Toksöz, et al., 1976). By substituting the density and bulk modulus of water for air in our non-framework model it should be possible to predict saturated V_p. Tosaya and Nur (Tosaya and Nur, 1982) published an empirical relationship of V_p, porosity, and clay content measured at 400 bars effective pressure. That relationship is given as:

$$V_p = -0.024Cl - 0.086\varphi + 5.8\ ,$$

where Cl = volume of clay in %, φ = porosity in %, and V_p is in km/sec. Because they used point counting to determine clay content, the clay term is equivalent to the matrix volume + microporosity of our model. A logical test is to see if the model, using water as a pore fluid, will predict approximately the empirical coefficients of Tosaya and Nur (Tosaya and Nur, 1982).

As an initial step the coefficient of the φ term is considered first. An average pore distribution of 15% connective and 85% intergranular is chosen based on our samples. Velocities of saturated sandstones of varying porosity are calculated with this pore type distribution, using $\alpha_I = 0.225$ and $\alpha_C = 0.05$; the results of the model are shown in figure 11. A linear regression through the predicted values yields $dV_p / d\varphi = -0.072$, a 15% difference from the -.086 value of Tosaya and Nur (Tosaya and Nur, 1982). However, the model contained a single pore aspect ratio distribution whereas the sample set presumably contains many different distributions. Were the amount of connective pores to increase only a few additional percent the model could match the φ coefficients of the measured data.

Modeling of the clay coefficient is more difficult. The dry model suggests that the clays are decoupled from the framework of the sample, cushioned by air in pores of aspect ratio 0.225. Modeling water filled pores of $\alpha = 0.225$ with increasing volume, results in $dV_p / dCl = -0.053$, a factor of two larger than the -0.024 of the empirical equation (Tosaya and Nur, 1982). The difference would appear to be in the assumption of decoupling. Because water transmits stress more effectively than air, the water-clay mix in the pore space should be regarded as a compound pore filing material, influenced by the moduli of both water and clay. Spherical pore aspect ratios (α=1.0) were used to model the 50% clay-50% water pore filling. For the clay grains values of $K = 0.44Mb$, $\mu = 0.35Mb$, and $\rho = 2.72$ gm/cc were used since clay moduli and the effects of swelling due to saturation are not known. Relatively "soft" clay moduli were chosen arbitrarily, however it should be kept in mind that the aspect ratio of the pores containing the clay is the dominant factor in the velocity calculations. Results of the model are effective moduli for the pore filling of K = 0.17Mb, $\mu = 0.12Mb$, ρ = 1.86 gm/cc. Velocities of pores with $\alpha = 0.225$ filled with the water-clay mixture are modeled in figure 12. A regression of the predicted values yields $dV_p / dCl = -0.021$, slightly more than 10% different than the empirical result of -0.024.

This result reinforces the concept of the role of clays in sandstone velocity. Although the clay in saturated samples cannot be totally ignored, it's effect on velocity can still be adequately explained as a result of a modification of the non-framework volume of the rock and not a framework effect. In saturated samples clays alter the moduli of the pore filling material, not the framework moduli.

CONCLUSIONS

Direct observations of pore space combined with aspect ratio modeling can be a very effective tool in explaining sandstone behavior. Velocities for a wide variety of sandstones can be predicted using simple observed pore type criteria.

(1) Compressional wave velocity in sandstones is best modeled by considering total non-framework (pore and matrix) volume rather than porosity, which includes only void space. Clay in sandstone does not change the non-framework volume, only the porosity.

(2) In saturated sandstones clay not only acts to fill non-framework volume, but also modifies the moduli of the pore filling material. The effect of the presence of clays in either dry or saturated sandstones can be modeled without changing any of the framework parameters.

ACKNOWLEDGEMENTS

This research was supported by a Schlumberger Post-Doctoral Fellowship for R. Wilkens at M.I.T. and a grant from the Schlumberger- Doll Research Center to G. Simmons. C.H. Cheng and M.N. Toksöz provided valuable guidance during the modeling and analysis of the data. Liz Henderson prepared the manuscript and Sue Turbak assisted in the preparation of the figures.

REFERENCES

Pittman, E.D. The pore geometries of reservoir rocks:in Johnson, D.C. and Sen, P.N., eds., Physics and Chemistry of Porous Media, American Institute of Physics Conf. Proc. 107, N.Y., 223 (1984).

Seeburger, D.A. and Nur, A. A pore space model for rock permeability and bulk modulus: J. Geophys. Res., v.89, 527-536 (1984).

Wyllie, M.R., Gregory, A.R., and Gardner, L.W. Elastic wave velocities in heterogeneous and porous media: Geophysics, v. 21, 41-70 (1956).

Wyllie, M.R., Gregory, A.R., and Gardner, L.W. An experimental investigation of factors affecting elastic wave velocities in porous media: Geophysics, v. 23, 459-493 (1958).

Birch, F. The velocity of compressional waves in rocks to 10 kilobars, 1: J. Geophys. Res., v. 65, 1083-1102 (1960).

Birch, F. The velocity of compressional waves in rocks to 10 kilobars, 2: J. Geophys, Res., v. 66, 2199-2224 (1961).

Walsh, J.B. The effect of cracks on the compressibility of rocks: J. Geophys. Res., v. 70, 381,389 (1965).

Walsh, J.B. New analysis of attenuation in partially melted rocks: J. Geophys. Res., v. 74, 4333-4337 (1969).

Pittman, E.D. and Duschatko, E. Use of pore casts and scanning electron microscope to study pore geometry: J. Sed. Pet., v. 40, 1153-1157 (1970).

Timur, A., Hempkins, W.B., and Weinbrandt, R.M. Scanning electron microscope study of pore systems in rocks: J. Geophys. Res., v. 76, 4932-4948 (1971).

Kuster, G.T. and Toksöz, M.N. Velocity and attenuation cf seismic waves in two phase media; Part I. Theoretical formulations: Geophysics, v. 39, 587-606 (1974a).

Kuster, G.T. and Toksöz, M.N. Velocity and attenuation of seismic waves in two phase media; Part II. Experimental results: Geophysics, v. 39, 607-618 (1974b).

O'Connell, R.J. and Budiansky, B. Seismic velocities in dry and saturated cracked solids: J. Geophys. Res., v. 79, 5412-5426 (1974).

Cheng, C.H. and Toksöz, M.N. Inversion of seismic velocities for the pore aspect ratio

spectrum of a rock, J. Geophys. Res., v. 84, 7533-7544 (1979).

De Martini, D.C., Beard, D.C., Danburg, J.S., and Robinson, J.H. Variation of seismic velocities in sandstones and limestones with lithlogy and pre fluid at simulated *in-situ* conditions: Proc. E.G.P.C. Exploration Seminar (Nov. 15-17, 1976).

Tosaya, C. and Nur, A. Effects of diagenesis and clays on compressional velocities in rocks: Geophys. Res. Lett., v. 9, 5-8 (1982).

Kowallis, B.J., Jones, L.E.A., and Wang, H.F. Velocity-porosity-clay content systematics of poorly-consolidated sandstones: J. Geophys. Res., in press (1985).

Caruso, L., Simmons, G., and Wilkens, R. The physical properties of a set of sandstones, I: The samples: submitted to Geophysics (1985).

Selley, R.C. An Introduction to Sedimentology, Academic Press, N.Y., 417 (1982).

Toksöz, M.N., Cheng, C.H., and Timur, A. Velocities of seismic waves in porous rocks: Geophysics, v.41, 621-645 (1976).

Wilkens, R.H., Simmons, G., and Caruso, L. The ratio V_p / V_s as a discriminant of composition for siliceous limestones: Geophysics, Nov. (1984).

Wissler, T.M. and Simmons, G. Permanent and elastic strains in sandstones to 200 MPa: submitted to International Jnl. Rock Mech (1985).

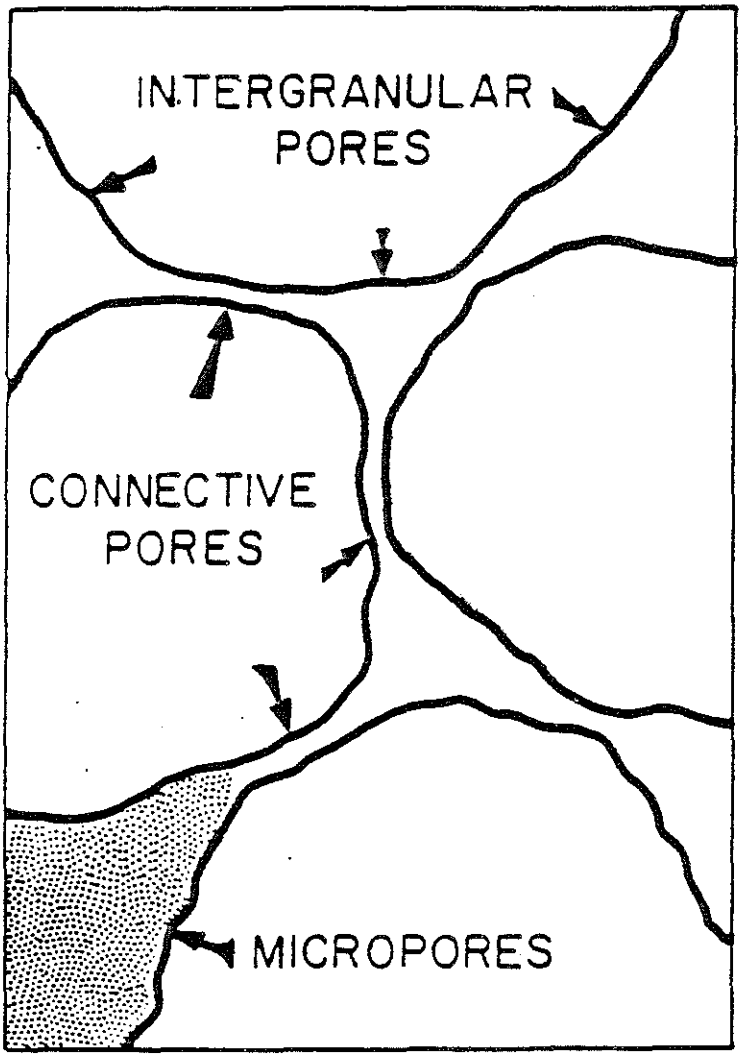

Fig. 1. (a) Schematic of pore geometry classification used in this study. intergranular pores are large aspect ratio pores containing no filling material. Connective pores are low aspect ratio crack-like pores. Micropores are the void spaces within matrix regions.

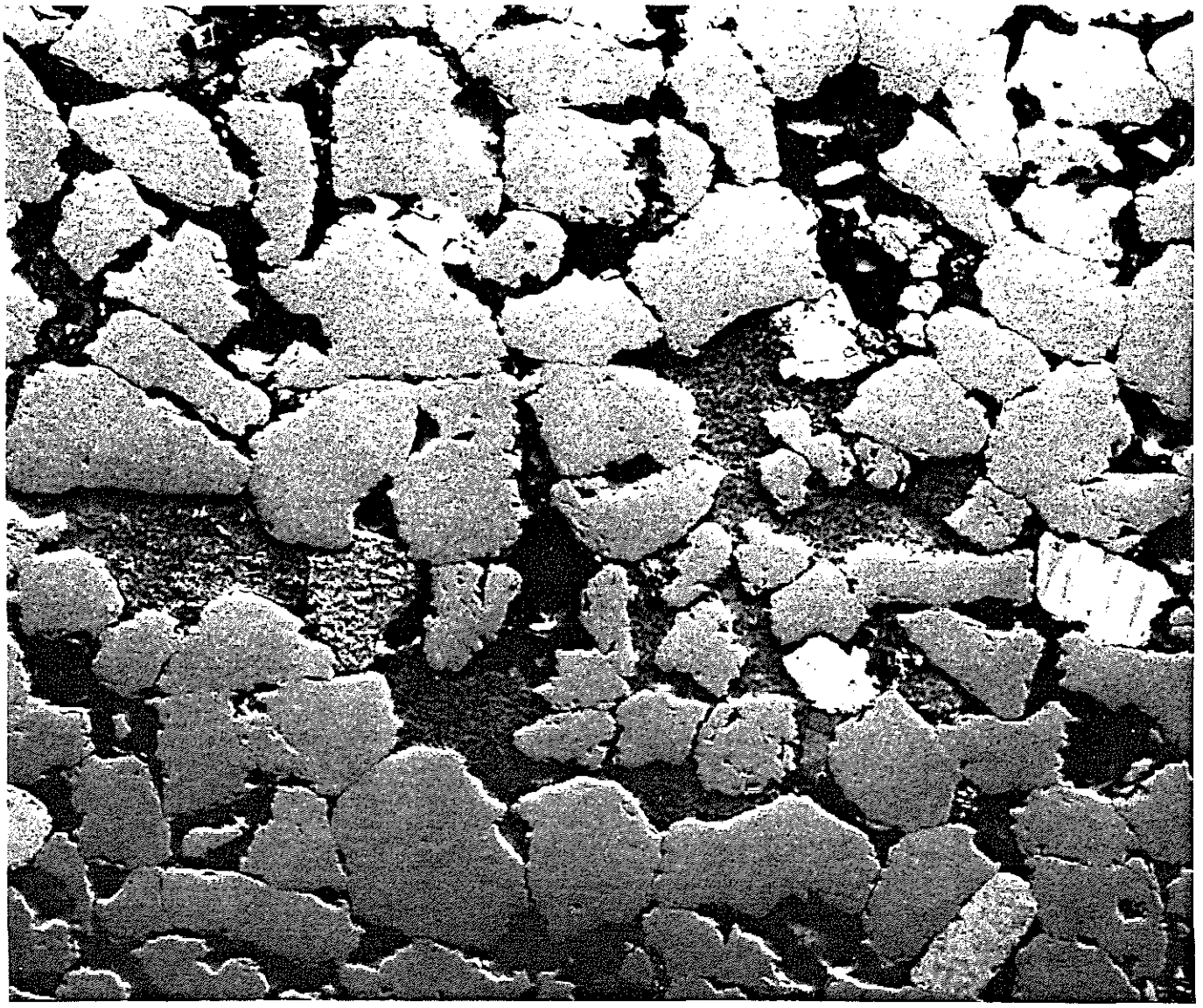

Fig. 1. (b) Back scattered electron image from scanning electron microscope of polished, impregnated section. Open (epoxy filled) pores are black. Mottled gray areas are matrix regions, predominantly kaolinite. Quartz framework grains are grey and occasional bright grains are feldspar. Scale bar is 500 microns.

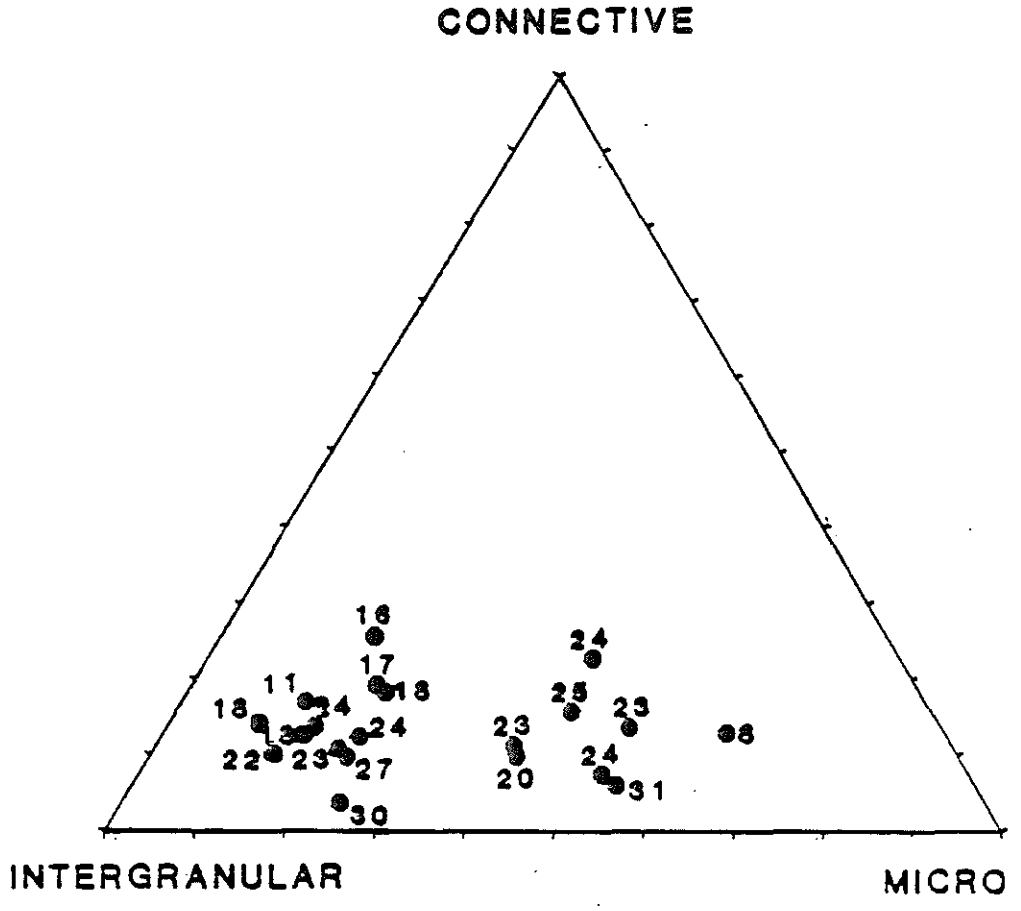

Fig. 2. Distribution of pore geometry for sandstones used in this study displayed on ternary diagram. Values are of average measured porosity from 3 cores of each sandstone.

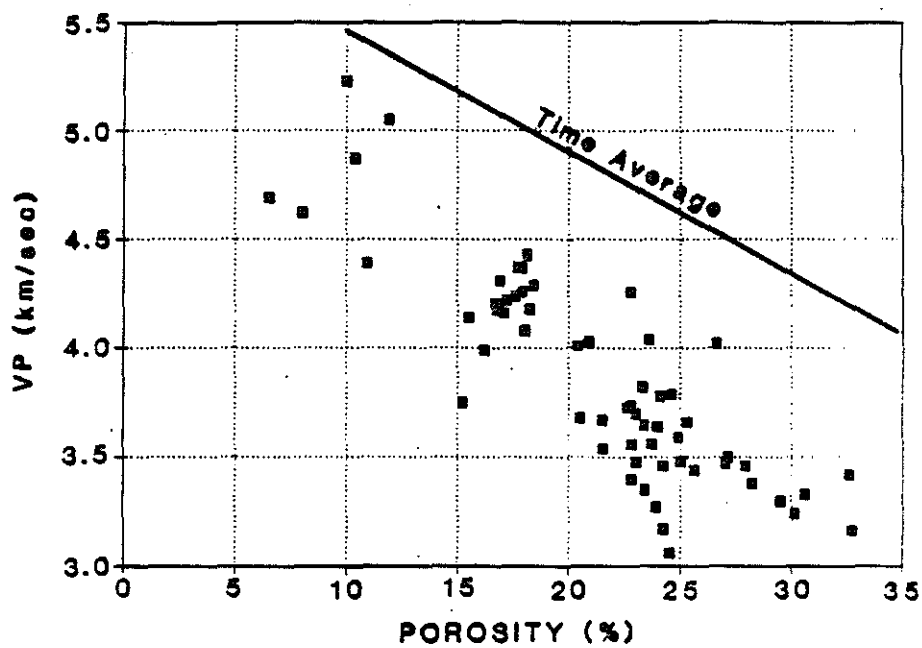

Fig. 3. Values of compressional wave velocity (V_p) at 0.5 kb plotted versus porosity for each of three dry cores from sandstones used in this study. Time average line is calculated using average V_p of single crystal quartz and air.

Figure 4a

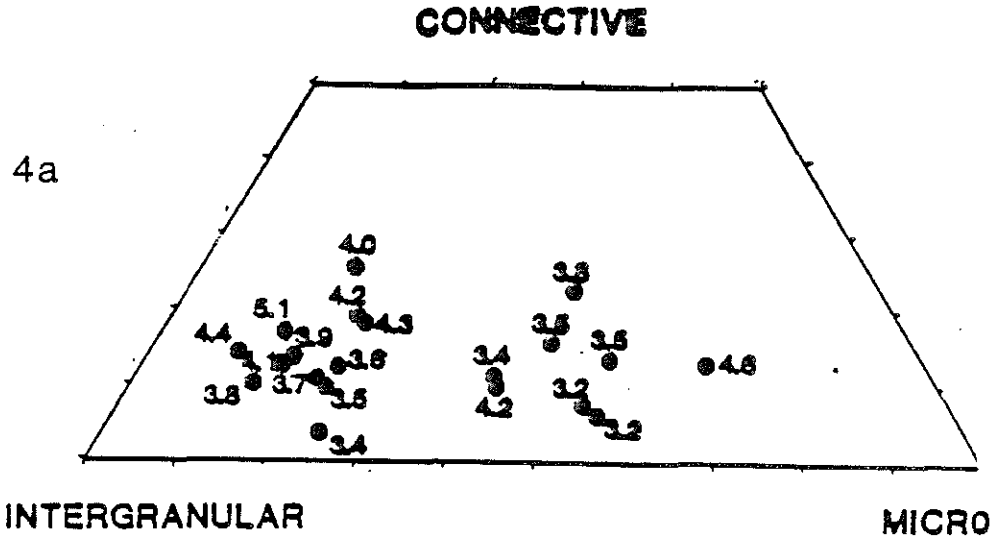

Figure 4b

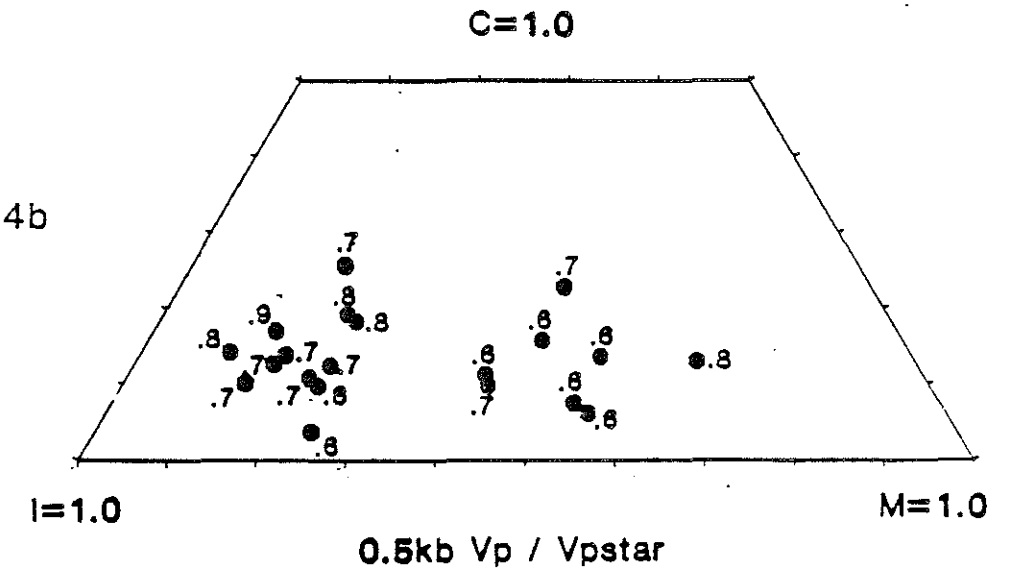

Fig. 4. (a) Average V_p (km/sec) measured at 0.5 kb confining pressure for dry cores. (b) Ratio of measured V_p values from (a) to modeled values assuming spherical pores (α = 1.0) and quartz framework.

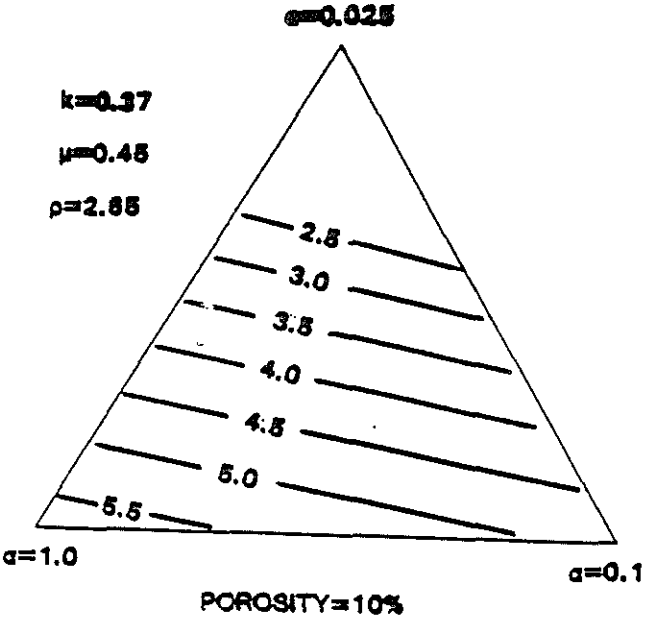

Figure 5a

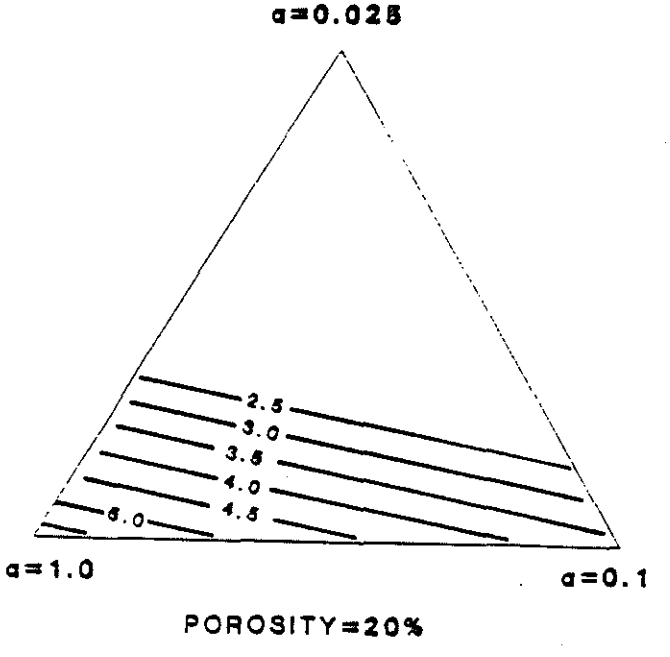

Figure 5b

Fig. 5. (a) Theoretical V_p contours (km/sec) for sandstone of 10% total porosity distributed between aspect ratios of 1.0, 0.1, and 0.025. (b) Same as (a) for sandstone of 20% total porosity.

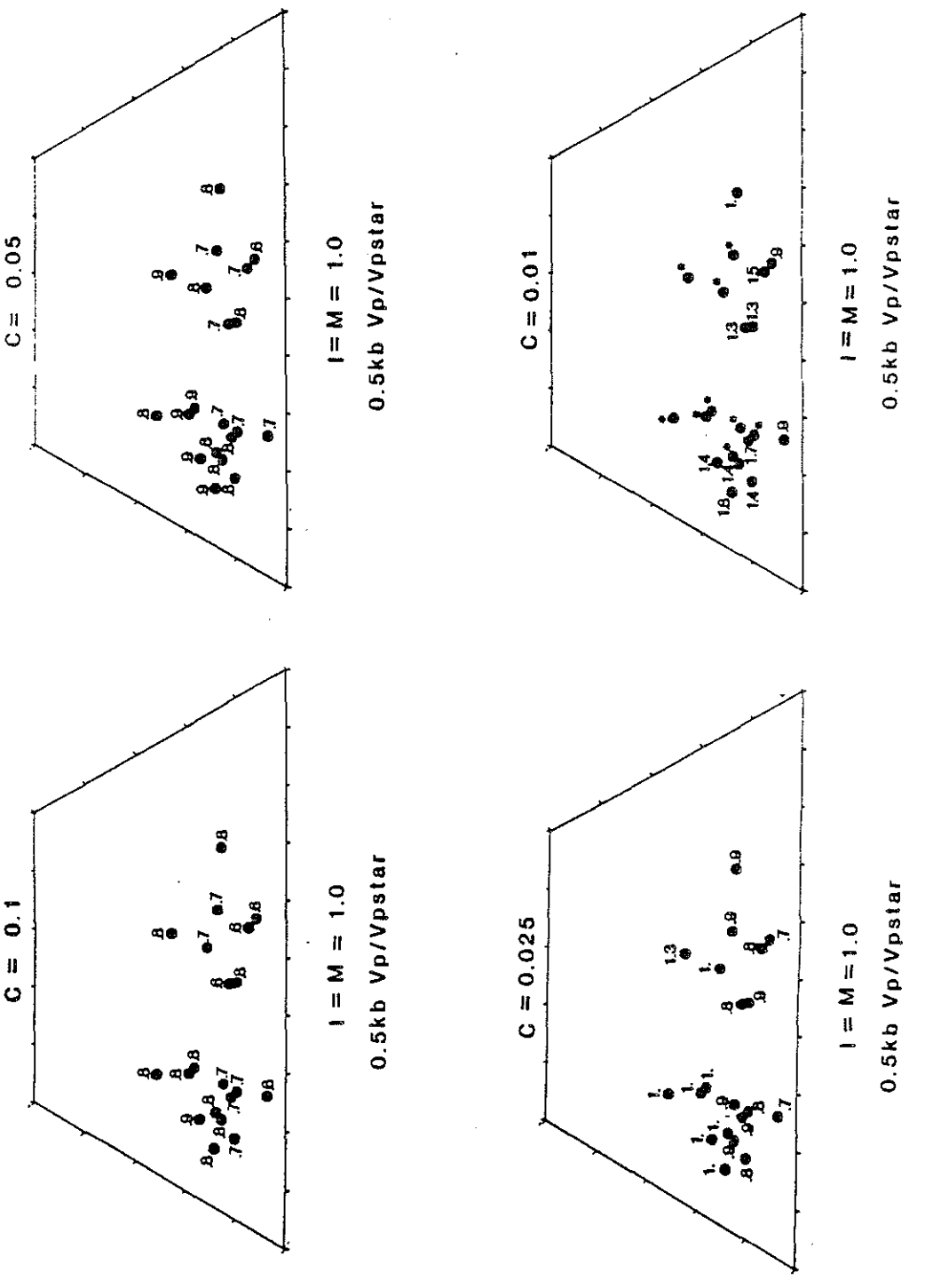

Fig. 6. Ratio of measured V_p values at 0.5 kb confining pressure to predicted values assuming spherical (α = 1.0) intergranular and micropores, and varying connective pore aspect ratio from 0.1 to 0.01.

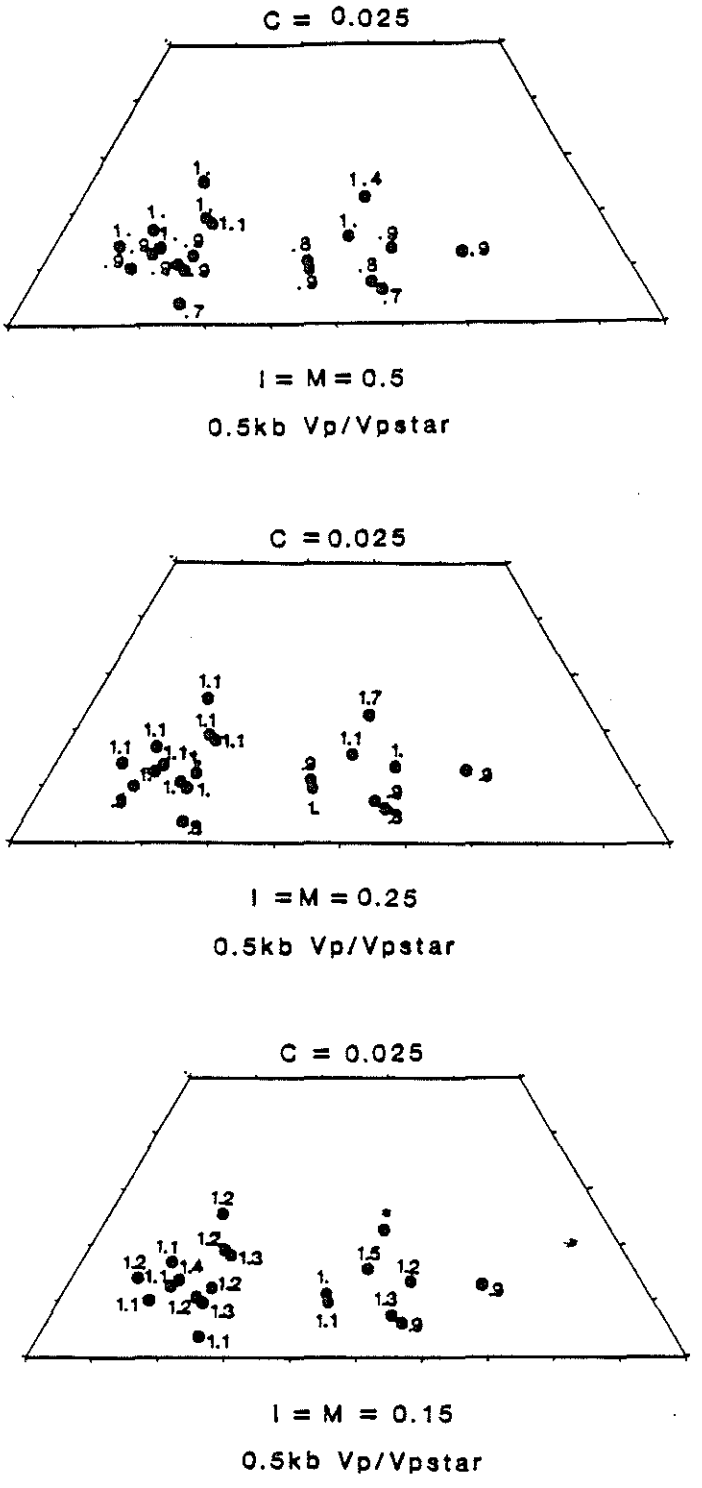

Fig. 7. Ratio of measured V_p values at 0.5 kb confining pressure to predicted values assuming constant connective pore aspect ratio of 0.025 and varying intergranular and micropore aspect ratios from 0.5 to 0.15.

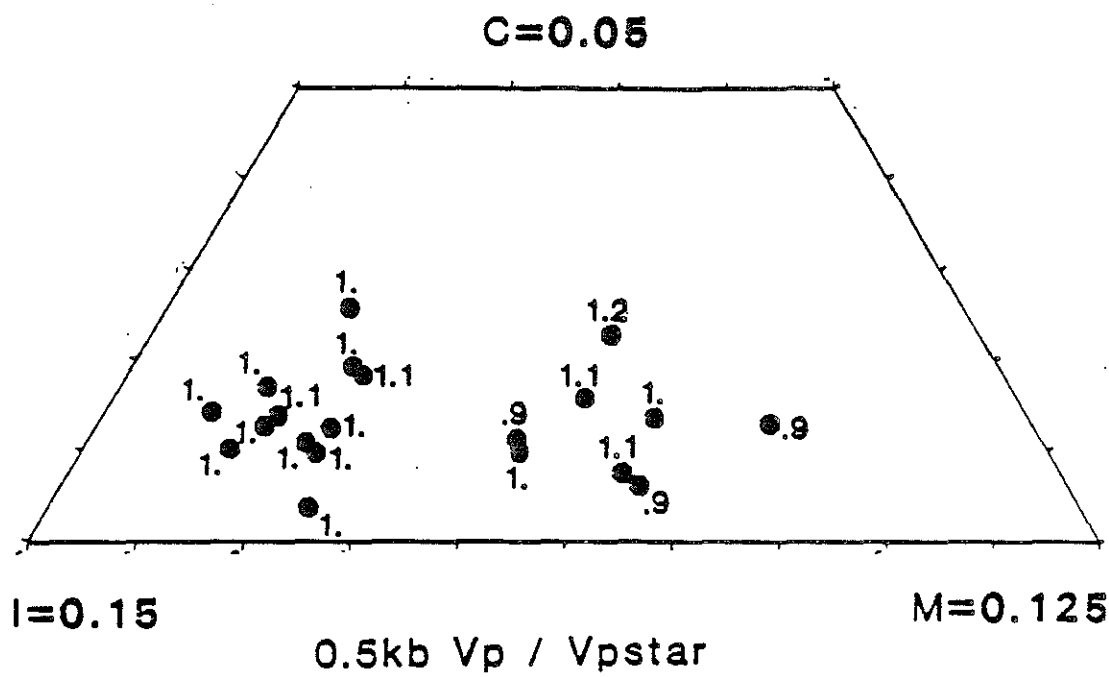

Fig. 8. Ratio of measured V_p values at 0.5 kb confining pressure to predicted values assuming connective pore aspect ratio of 0.025, intergranular pore aspect ratio of 0.15, and micropore aspect ratio of 0.125.

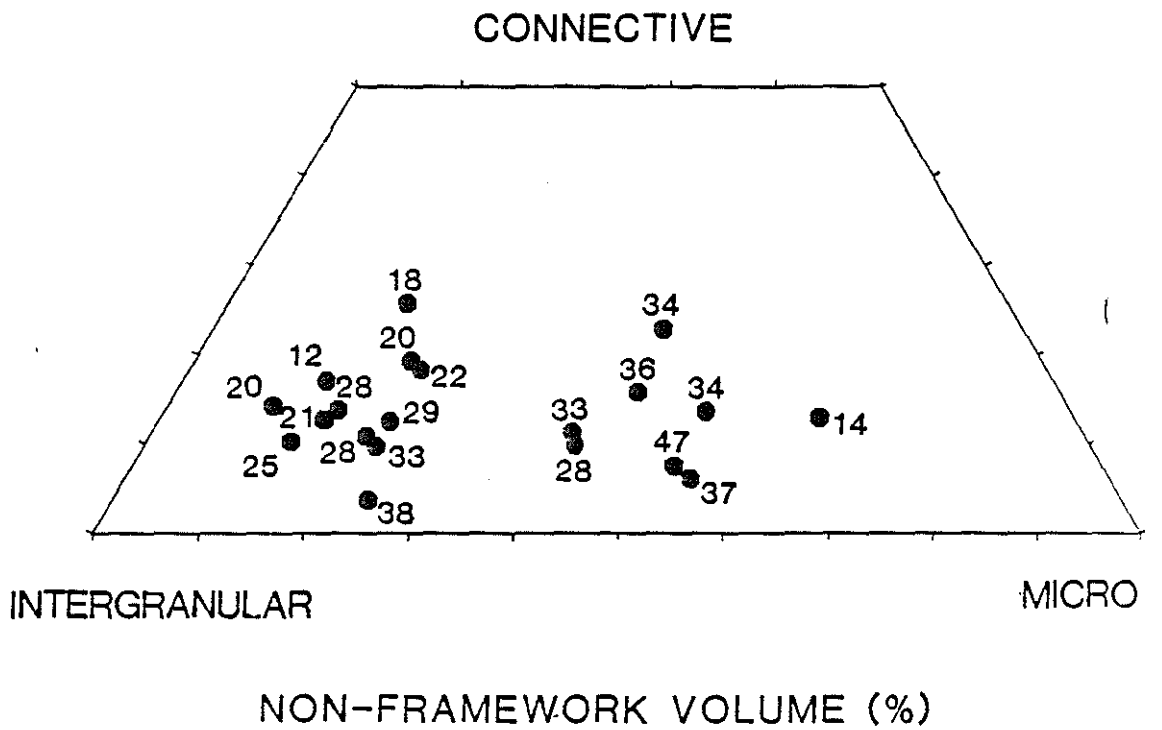

Fig. 9. Values of non-framework volume equal to void volume (porosity) plus volume of matrix (pore filling material).

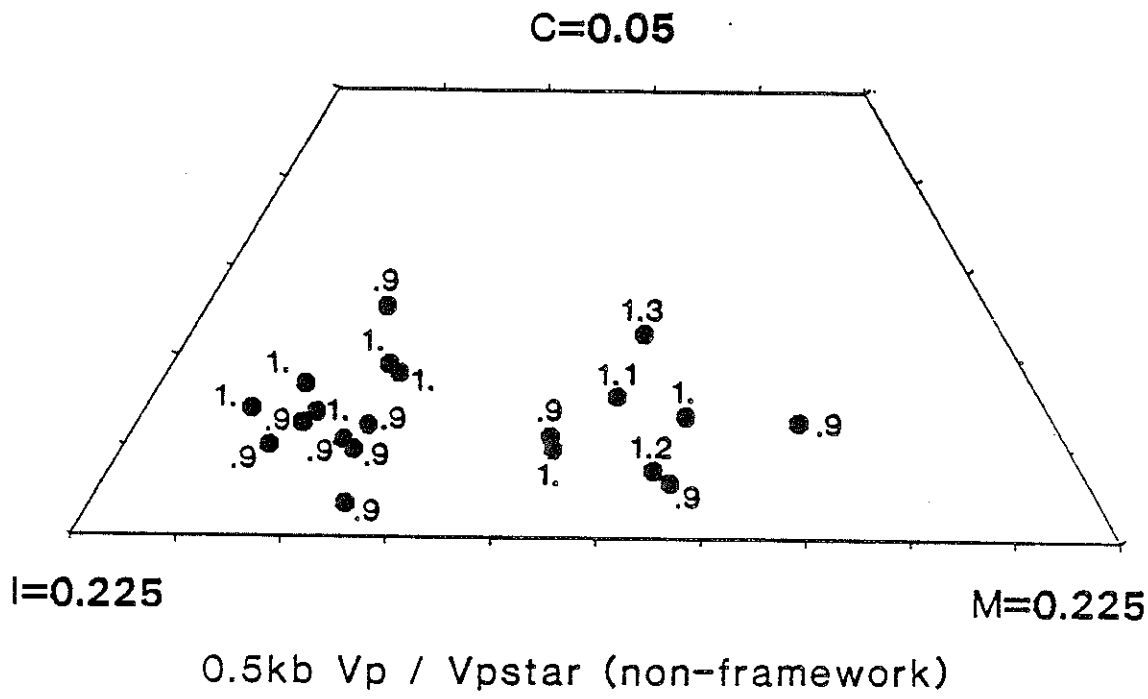

Fig. 10. Ratio of measured V_p values at 0.5 kb confining pressure to predicted values using non-framework model and assuming connective pore aspect ratio of 0.05, intergranular and microporosity zone aspect ratios of 0.225.

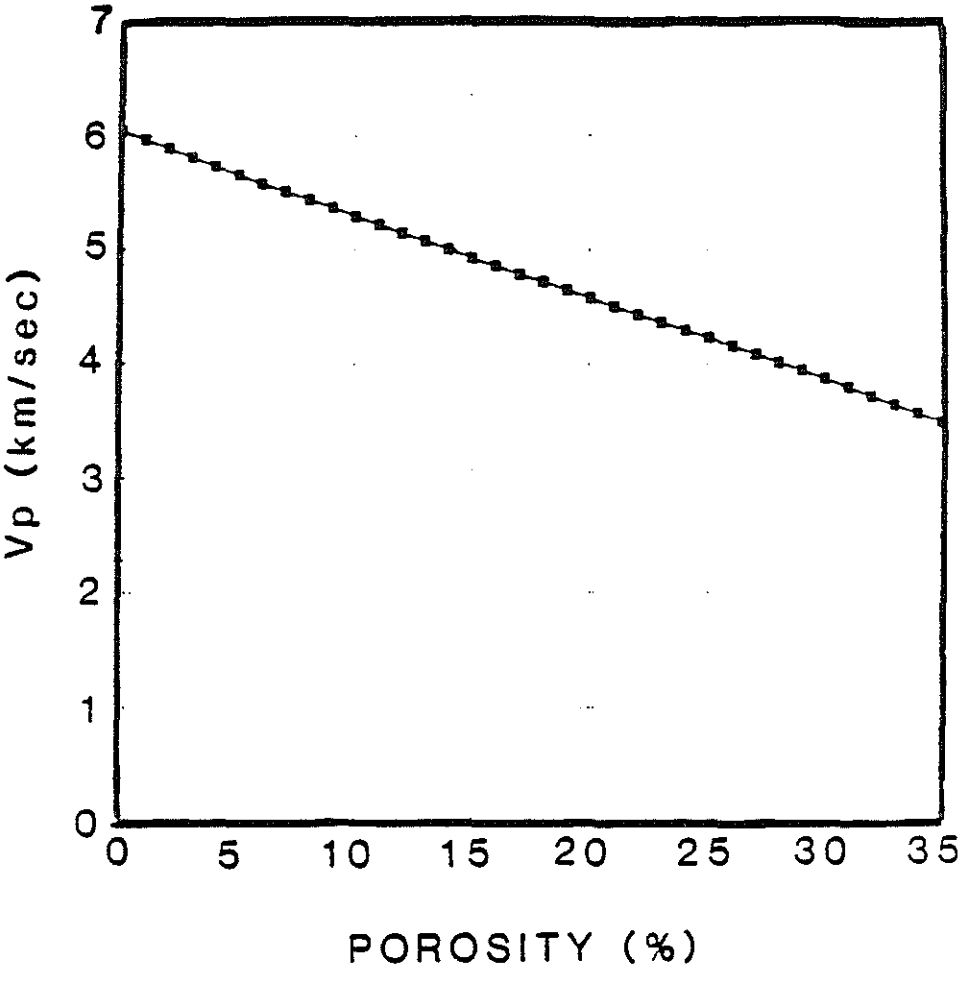

Fig. 11. Predicted values of V_p versus porosity for water saturated sandstone assuming 85% intergranular pores (α = 0.225) and 15% connective pores (α = 0.05).

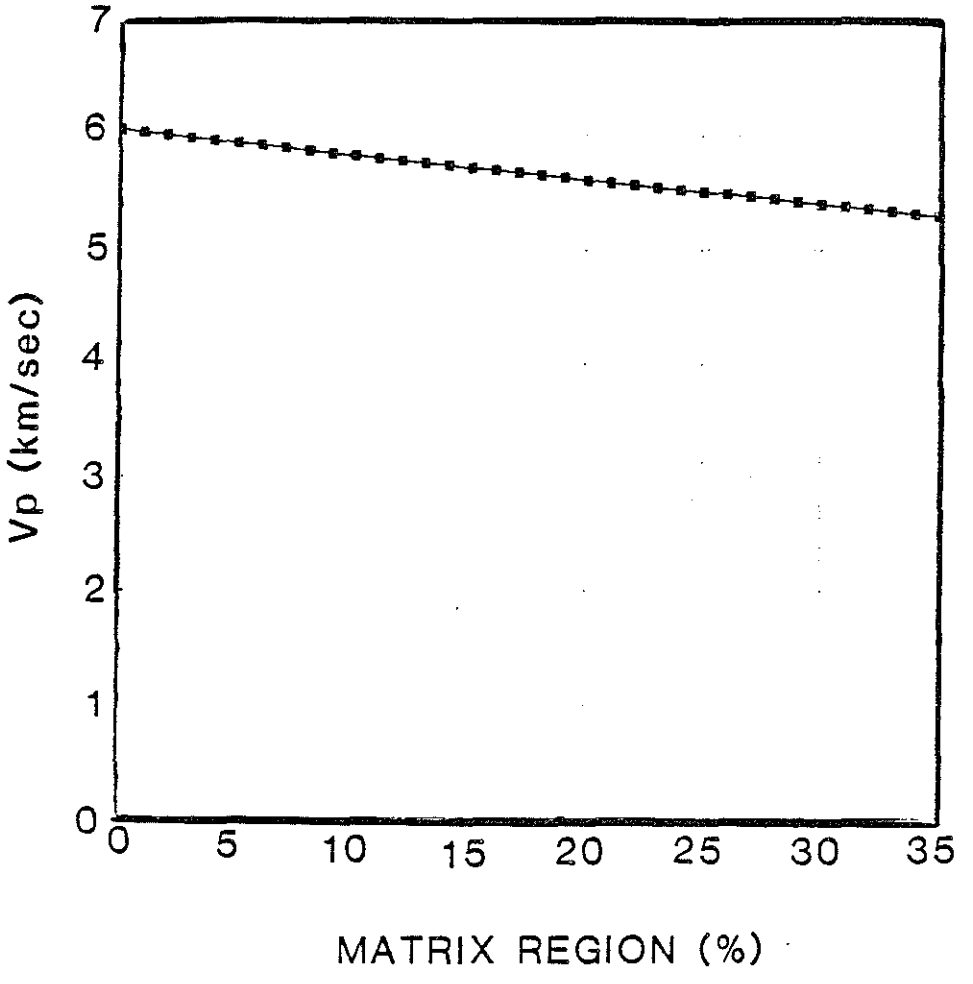

Fig. 12. Predicted values of V_p versus matrix region volume for water saturated sandstone assuming aspect ratio of 0.225; effective moduli of pore filling K = 0.17Mb, $\mu = 0.12kb$, ρ = 1.82 gm/cc.